BioOne COMPLETE

Climatic Influences on Wood Anatomy and Tree-Ring Features of Great Basin Conifers at a New Mountain Observatory

Authors: Ziaco, Emanuele, Biondi, Franco, Rossi, Sergio, and Deslauriers, Annie

APPLICATION ARTICLE

CLIMATIC INFLUENCES ON WOOD ANATOMY AND TREE-RING FEATURES OF GREAT BASIN CONIFERS AT A NEW MOUNTAIN OBSERVATORY[1]

EMANUELE ZIACO[2], FRANCO BIONDI[2,3,5], SERGIO ROSSI[4], AND ANNIE DESLAURIERS[4]

[2]DendroLab, University of Nevada, Reno, Nevada 89557 USA; [3]Harvard Forest, Petersham, Massachusetts 01366 USA; and [4]Département des Sciences Fondamentales, Université du Québec à Chicoutimi, Chicoutimi, Québec G7H2B1, Canada

- *Premise of the study:* A network of mountain observing stations has been installed in the Great Basin of North America. Nev-CAN (Nevada Climate-ecohydrological Assessment Network), which spans a latitudinal range of 2.5° and two elevation ranges of about 2000 m each, enabled us to investigate tree growth in relation to climate.
- *Methods:* We analyzed wood anatomy and tree-ring characteristics of four conifer species in response to different levels of water availability by comparing a low- and a high-elevation population. Chronologies of earlywood and latewood widths, as well as cellular parameters, were developed from the year 2000 to 2012.
- *Results:* At the southern (drier and warmer) sites, *Pinus monophylla* had smaller cell lumen, tracheid diameter, and cell wall thickness. *Pinus monophylla* and *P. flexilis* showed bigger cellular elements at the higher elevations, whereas the opposite pattern was found in *Picea engelmannii* and *Pinus longaeva*. When all species and sites were pooled together, stem diameter was positively related with earlywood anatomical parameters.
- *Discussion:* We have provided a glimpse of the applications that NevCAN, as a new scientific tool, could allow in the general field of botany. In particular, we were able to investigate how differences in water stress related to elevation lead to changes in xylem anatomy.

Key words: elevation-latitude gradients; NevCAN; *Picea engelmannii*; *Pinus flexilis*; *Pinus longaeva*; *Pinus monophylla*; tracheid size.

Responses of ecosystems to climate change are complex because of multiple confounding factors acting together over a range of temporal and spatial scales (Sistla et al., 2013; Keenan et al., 2014). Natural climate gradients found along mountain slopes provide an effective way to study combined biotic and abiotic effects on ecological patterns and processes (Raich et al., 1997; King et al., 2013). As climatic conditions change with elevation, they act as a driving force for vegetation, for example, by shaping forest distribution (Peñuelas and Boada, 2003), turnover rates (Stephenson and van Mantgem, 2005), and forest structure (Holeksa et al., 2007), with resulting changes in dominant species that lead to the identification of bioclimatic zones (Di Filippo et al., 2007; Crausbay and Hotchkiss, 2010). Overall, identifying ecological gradients is one of the most powerful analytical strategies for field-based investigations on environmental controls of vegetation patterns (Whittaker, 1967).

A gradient-based approach has been used to study eco-hydro-climatic drivers of tree growth in a variety of North American settings. The focus of published research has ranged from the relatively flat forested lands in Florida (Foster and Brooks, 2001) and the large expanse of the boreal biome in Quebec (Rossi et al., 2014a) to the topographically complex forest landscapes of California (Bekker and Taylor, 2001), Arizona (Fritts et al., 1965), New Mexico (Padien and Lajtha, 1992), and Nevada (LaMarche, 1974). Recently there has been an added emphasis on employing altitudinal-latitudinal gradients to study climate–growth relationships at finer spatial and temporal scales. Processes have therefore been analyzed at the individual tree level (Galván et al., 2012; van der Maaten-Theunissen and Bouriaud, 2012), using microscopic features (St-Germain and Krause, 2008; Rossi et al., 2014b), and at intra-annual time scales (de Luis et al., 2011; DeSoto et al., 2011). This increased resolution is associated with a demand for site-specific data, and newly installed networks of

instrumental stations have been used to evaluate the effects of local climate on xylem formation (Deslauriers et al., 2008), tree-ring properties (Krause et al., 2010), timber quality (Rossi et al., 2014b), and ecophysiological responses of tree species from different provenances (Reinhardt et al., 2011).

In the Great Basin of North America, where climate is overall quite dry (Grayson, 2011), elevation is inversely correlated with temperature and directly correlated with precipitation (Houghton et al., 1975). A new mountain observatory composed of valley-to-mountain transects has been built in this region between 2010 and 2013 with state-of-the-art instrumentation to capture ecosystem dynamics in real time (Mensing et al., 2013). The Nevada Climate-ecohydrological Assessment Network (NevCAN) consists of stations equipped with a set of automated sensors that record climatic and environmental variables at subhourly time intervals. To represent biogeographic and macrosystem changes, two mountain ranges separated by about 2.5° latitude were selected. The southern site is an example of warmer and drier regions influenced by the North American Monsoon System; the northern location typifies areas dominated by cool-season precipitation and snowpack dynamics. At either location, elevation gradients span about 2000 m, thus enabling researchers to perform field studies on ecosystem processes with unprecedented detail (Johnson et al., 2014). Because of the availability of high-resolution climatic data (hourly to subhourly), detailed measurements of tree growth can be linked to intra-annual climatic events recorded by xylem rings and wood anatomy features.

Tree rings represent a unique archive of ecological and environmental information (Fritts, 2001). Dendrochronological proxy records have provided spatial and temporal indices of interannual climate variability over several centuries in all inhabited continents (Speer, 2010). Empirical relationships between tree rings and climate have also been investigated at the intra-annual level, e.g., for reconstructing summertime precipitation by means of latewood-width chronologies (Stahle et al., 2009; Griffin et al., 2013). A process-based understanding of the physiological mechanisms controlling the climatic response of woody species can be obtained using anatomical studies (Deslauriers et al., 2003; Fonti et al., 2010). In those investigations, the tree growing season is commonly sampled by means of microcores extracted at time intervals ranging from a few days to a couple of weeks. Developmental stages of xylem cells, and timing of their occurrence, can be recognized, thus revealing linear and nonlinear dynamics of xylem phenology (Rossi et al., 2013). Such intra-annual data make it possible to detect the consequences of short-term environmental signals on tree-ring formation and radial growth. In fact, microscopic wood traits (e.g., lumen area, cell diameter, wall thickness) respond to climatic and environmental conditions as much or even more, in some instances, than ring width (de Luis et al., 2011; Olano et al., 2012; Liang et al., 2013).

In conifers most of the wood is composed of tracheids, which simultaneously provide vascular transport and mechanical support (Vaganov et al., 2006). Tracheid size has been found to be positively correlated with moisture availability at the time of cell formation (Vieira et al., 2009). The cross-sectional area (lumen) of tracheids, while providing water transport and being directly linked to the hydration of the plant, depends on complex mechanical and physiological trade-offs between structural development and resistance to drought (Sperry et al., 2006). Trees hold a high degree of plasticity, and are able to adjust newly formed annual tracheids to external conditions, so that variability recorded in tree rings can be used for retrospective studies of past hydraulic adjustments to water availability (Bryukhanova and Fonti, 2013). Because cellular parameters respond to environmental conditions at the time of their formation, they also present lower time-series autocorrelation than tree-ring width (Deslauriers and Morin, 2005).

Our overall objective is to determine the climatic factors that control radial growth in Great Basin conifers. The NevCAN transects enabled us to compare wood anatomy and tree-ring characteristics among species at different elevations and at locations (north and south) with distinct climatic regimes. By testing for the existence of common variability associated with different levels of water stress, we addressed the following questions: (a) Is there a connection between growing season climate and anatomical characteristics (e.g., lumen area and cell diameter) that are related to stem water transport?, (b) How are precipitation and air temperature variables linked with intra- or interspecific variations of tree-ring and anatomical parameters?, and (c) Are environmental signals in earlywood and latewood widths the same as for cellular features?

MATERIALS AND METHODS

Study area—The NevCAN northern transect (Fig. 1) is located in the Snake Range (east-central Nevada, close to the Utah border), while the southern transect is in the Sheep Range (southern Nevada, about 50 km north of Las Vegas). The northern transect consists of eight stations starting from 1755 m a.s.l. on the western side of the range, culminating at 3355 m a.s.l. near treeline, and ending at 1560 m a.s.l. on the eastern side of the range (Fig. 1; Table 1). Both private and public landowners are involved, including the Long Now Foundation (three sites), the Bureau of Land Management (three sites), Great Basin National Park (one site), and the Nevada Land Conservancy (one site). The southern transect consists of five stations, starting at 900 m a.s.l. and ending at 3015 m a.s.l. on land managed by the U.S. Fish and Wildlife Service, and often co-located with Natural Resources Conservation Service (NRCS) Soil Climate Analysis Network (SCAN) sites.

On the west side of the Snake Range, forest cover at the montane level is composed by *Pinus flexilis* E. James, *Pseudotsuga menziesii* (Mirb.) Franco, and *Abies concolor* Lindl. ex Hildebr.[1] Shrub layers are formed by mountain mahogany (*Cercocarpus ledifolius* Nutt.) and greenleaf manzanita (*Arctostaphylos patula* Greene). Near and at treeline, the dominant species is *Pinus longaeva* D. K. Bailey, mixed with scattered individuals of *Picea engelmannii* Parry ex Engelm. and *Pinus flexilis*. On the east side of the range, *Picea engelmannii* is the most abundant species, together with several large individuals of *Populus tremuloides* Michx. and some *Pinus flexilis*. At the Sheep Range, the lower elevations are occupied by woodlands composed of *Pinus monophylla* Torr. & Frém. and *Juniperus osteosperma* (Torr.) Little, while the montane site includes several large individuals of *Pinus ponderosa* var. *scopulorum* Engelm. together with *Pinus monophylla*.

Field collections—This study was conducted at five NevCAN sites (Table 1). Three sites were sampled at the Snake Range, namely the Subalpine West (Sna1-2, 3355 m a.s.l.; see below), the Subalpine East (Sna3, 3070 m a.s.l.), and the Montane West (Sna4, 2810 m a.s.l.). The Subalpine West site was subdivided in two parts, High (Sna1) and Low (Sna2), to represent two distinct groups of trees separated by about 10 m in elevation. Two sites were sampled at the Sheep Range, the Montane (She1, 2320 m a.s.l.) and the Pinyon-Juniper (She2, 2065 m a.s.l.). Four conifer species were analyzed, including Engelmann spruce (*Picea engelmannii* [abbreviation: PIEN]), bristlecone pine (*Pinus longaeva* [PILO]), limber pine (*Pinus flexilis* [PIFL]),

---

[1] Latin names are from the International Plant Names Index (IPNI; http://www.ipni.org/index.html).
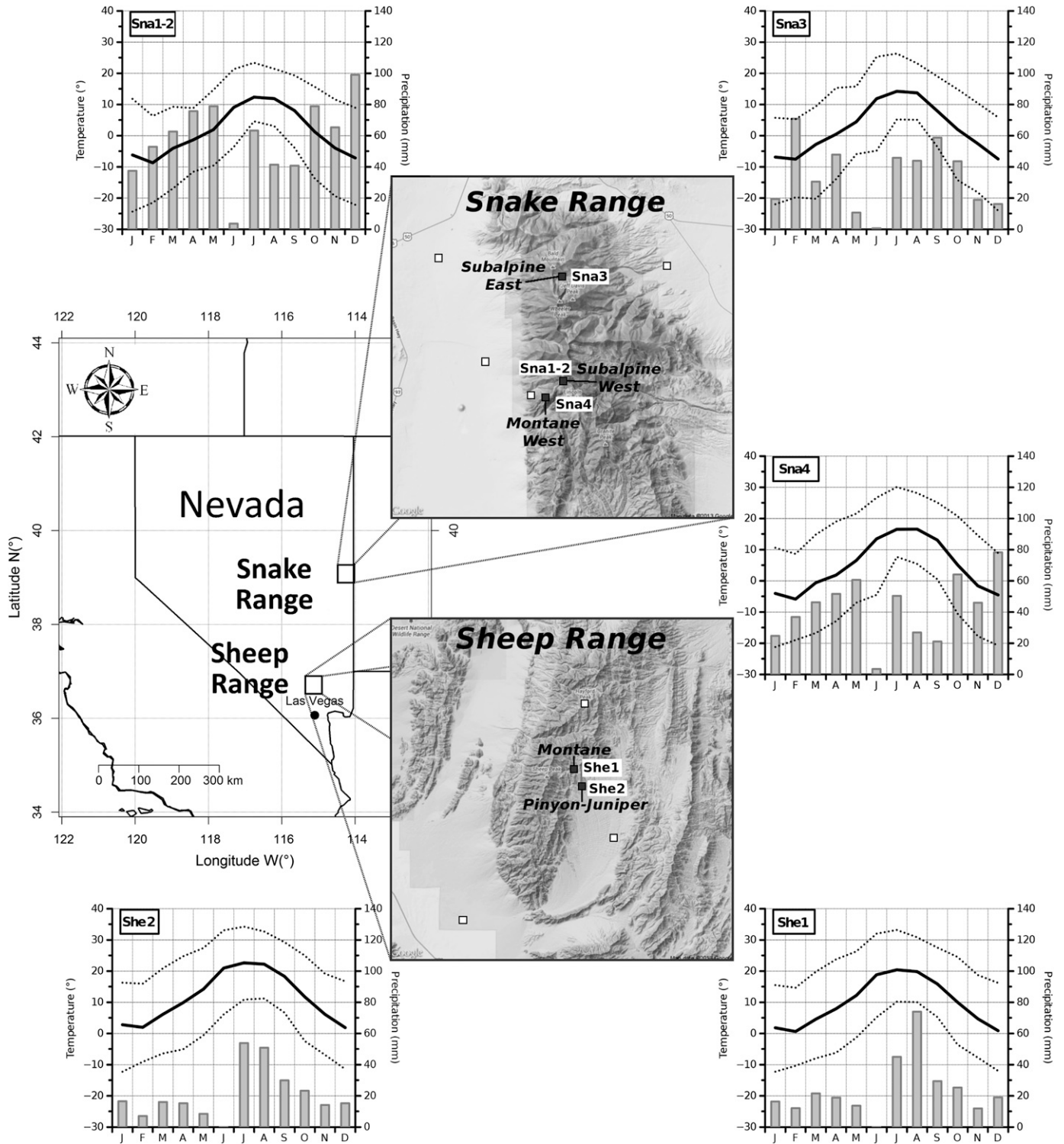
Fig. 1. Map of the study areas with climate diagrams showing mean monthly temperature (bold line), minimum and maximum monthly temperature (dotted lines), and total precipitation (vertical bars) recorded by the NevCAN stations during the 2010–2013 period. White squares represent NevCAN sites not sampled for this study.

and pinyon pine (*Pinus monophylla* [PIMO]). Each species occurred at two sites (Table 1). In the Snake Range (northern area), PILO was present at Sna1 and Sna2, PIEN at Sna1 and Sna3, and PIFL at Sna2 and Sna4. In the Sheep Range (southern area), PIMO occupied She1 and She2. Sampled stems were located in close proximity (10–15 m) of the meteorological station

that recorded climate parameters (air temperature at 2 m height; total liquid and solid precipitation) at each site.

A total of 57 trees were sampled between June and September 2013. Within each population, sampled trees had similar sizes (Table 1; diameter at breast height, or dbh, was measured ca. 1.3 m above ground level) to minimize the

TABLE 1. Summary information on study sites and sampled species.

Site name	Site code	Elevation, m a.s.l.	Species	Species acronym	No. of sampled trees	Avg. stem dbh, cm (range)[a]	Avg. tree height, m (range)
Snake Range							
Subalpine West High	Sna1	3360	*Pinus longaeva*	PILO	8	30 (15–34)	7 (5–10)
			Picea engelmannii	PIEN	4	43 (33–45)	12 (11–13)
Subalpine West Low	Sna2	3350	*Pinus longaeva*	PILO	8	35 (20–50)	9 (7–10)
			Pinus flexilis	PIFL	6	24 (17–35)	6 (4–8)
Subalpine East	Sna3	3070	*Picea engelmannii*	PIEN	6	47 (21–65)	11 (8–14)
Montane West	Sna4	2810	*Pinus flexilis*	PIFL	5	22 (7–30)	7 (4–7.5)
Sheep Range							
Montane	She1	2320	*Pinus monophylla*	PIMO	8	26 (16–38)	7 (5–8)
Pinyon-Juniper	She2	2065	*Pinus monophylla*	PIMO	12	20 (7–30)	4 (2–5)

[a] dbh = diameter at breast height (ca. 1.3 m above ground level).

effects of tree size on anatomical parameters (Anfodillo et al., 2012). The largest individuals were PIEN located at the western and eastern subalpine sites of the Snake Range (mean dbh was 43 and 47 cm, respectively). Wood microcores 1–2 mm wide and ca. 1 cm long were collected using a surgical bone-marrow needle or a Trephor (Rossi et al., 2006). Trees were sampled at breast height (about 1.3 m above ground level) whenever possible. In about 25% of cases, sampling took place at lower heights to avoid branch intersections and/or portions of the stem with scars or a strong leaning—hence possible reaction wood. After extraction, microcores were stored in a 50% ethanol solution to avoid tissue deterioration.

Sample preparation and measurement—In the laboratory, microcores were dehydrated with ethanol and PROTOCOL Safeclear II (Fisher Scientific, Waltham, Massachussetts, USA) and embedded in blocks of paraffin. Several transversal sections 8–10 μm thick were cut from each sample using a Leica rotary microtome (Leica Biosystems, Buffalo Grove, Illinois, USA), then permanently mounted on glass slides. Sections were stained with safranin (0.50% in water) and images were taken at 100–200× magnification with a digital camera mounted on a microscope. Images were analyzed with WinCELL software (Guay, 2013).

Each microcore included several xylem layers, from 3–4 in fast-growing trees (PIEN at Sna3) up to 40–50 in slow-growing ones (PILO at Sna1-2). The average number of tree rings in all microcores for all species was 13, so the period 2000–2012 was selected for comparison purposes, with the only exception being PIEN at Sna1, where year 2000 was not available. Tree rings were visually cross-dated (Douglass, 1941) to assign each radial growth increment to the year of formation. Anatomical and tree-ring parameters were measured along three lines within each annual ring (Deslauriers et al., 2003). Anatomical parameters consisted of lumen area (la), cell diameter (cd), and average cell wall thickness (wt; Appendix S1); ring parameters were earlywood width (EW), latewood width (LW), and total ring width (RW). EW and LW were measured by averaging the sum of tracheid diameters classified as earlywood or latewood along the three lines.

The latewood definition based on anatomical parameters that was provided by Mork has been interpreted in two different ways by different authors (Denne, 1988). In addition, other criteria to separate earlywood and latewood have been proposed when using densitometry traces (Franceschini et al., 2013). Given the anatomical emphasis of this study, we followed the criterion used by the Win-CELL software (Guay, 2013), which is equivalent to "formula 2" in Denne (1988). Earlywood and latewood were also separated according to the visual identification of the first onset of lumen contraction within a ring (Stahle et al., 2009). Results based on this method showed a very high linear correlation ($R^2 = 0.98$) with the anatomical definition, which was then used for further analyses, as it is less prone to subjective interpretations.

Data analysis—Intraspecific features were analyzed pairwise, comparing trees of the same species growing at different elevations and, for PIEN, slope exposure (west vs. east). Yearly profiles of lumen area, cell diameter, and wall thickness were standardized and averaged to create tracheidograms of anatomical parameters for the period 2000–2012. A tracheidogram displays the intra-annual variation of an anatomical parameter in the radial direction, according to its relative position (rank) within the ring (Vaganov, 1990). Standardized tracheidograms were computed using the *tgram* package for the R software environment (R Development Core Team, 2012), using a normalized number of

30 cells per ring (Vaganov et al., 2006). Tukey's biweight mean (Mosteller and Tukey, 1977) from the *dplR* package (Bunn et al., 2014) was applied to reduce the effect of outliers. Year-to-year changes in anatomical parameters were analyzed by species.

Anatomical parameters were computed separately for earlywood and latewood (e.g., lumen area of earlywood tracheids = laEW, lumen area of latewood tracheids = laLW; see Table 2). We quantified the effects of stem size on anatomical parameters by testing earlywood and latewood anatomical features against dbh. Mean chronologies of earlywood and latewood widths and their related microscopic features (lumen area, cell diameter, and wall thickness) for the period 2000–2012 were computed by species and site. Analysis of variance (ANOVA) was performed on earlywood and latewood anatomical parameters to test for differences related to elevation. Levene's test (Brown and Forsythe, 1974) was used to check the homogeneity of variance of anatomical features. The relationship between tree-ring (EW and LW) and anatomical parameters was tested for each species and site by linear correlation analysis and by graphical comparisons between normalized chronologies. Anatomical parameters of earlywood (laEW, cdEW, and wtEW) and latewood (laLW, cdLW, and wtLW) were compared to climatic variables: mean air temperature and total precipitation for spring (April–June) and summer (July–September), respectively.

RESULTS

Climatic regime—Climatic data recorded by the NevCAN stations during the period 2010–2013 showed higher mean annual temperature at the Sheep Range (9.8°C and 11.6°C at She1 and She2) compared to the Snake Range (1.1°C, 2.3°C, and 4.7°C at Sna1-2, Sna3, and Sna4, respectively). The summer months (June–August) were the warmest ones, but water stress varied among sites. The southern area was drier, and its precipitation regime was influenced by the North American Monsoon System (Adams and Comrie, 1997). Summer precipitation (July–September) accounted for more than 50% of total annual precipitation at She1 and She2, whereas at the

TABLE 2. Abbreviations of tree-ring and anatomical parameters measured in this study.

Parameter	Total ring	Earlywood	Latewood
Tree-ring parameters			
Ring-width, mm	RW		
Earlywood width, mm		EW	
Latewood width, mm			LW
Anatomical parameters			
Lumen area, μm²		laEW	laLW
Cell diameter, μm		cdEW	cdLW
Wall thickness, μm		wtEW	wtLW

Snake Range fall–spring precipitation (October–May) supplied about 80% of total annual solid and liquid precipitation, in particular on the western slope (Fig. 1). On the eastern side of the Snake Range (Sna3), total annual precipitation was lower compared with the western side, but summer precipitation was more abundant (36% of total annual precipitation). At all sites June was the driest month, with almost no precipitation (Fig. 1).

Tracheidograms—Standardized tracheidograms of anatomical features (lumen area, cell diameter, wall thickness) in the period 2000–2012 showed differences related to latitude, elevation, and slope exposure (Appendix S2). PIMO, which was sampled at the southern site, had smaller lumen areas, tracheid diameter, and wall thickness than the northern species, with the exception of lumen area in PILO, which was similar (Fig. 2). At the intraspecific level, both PIMO and

PIFL trees growing at the higher elevations showed larger cellular elements. Tracheid size of PIMO was constantly greater during 2000–2012 at She1 compared to She2 (median la was 433 μm^2 and 333 μm^2, respectively; mean cd was 23.2 μm and 19.5 μm, respectively). At the higher site, PIFL had larger tracheids in nine out of 13 years (median la was 601 μm^2 at Sna2 and 585 μm^2 at Sna4) and cell diameter was larger in five out of 13 years (median cd was 29.4 μm and 29.6 μm at Sna2 and Sna4, respectively).

Tracheids of the other two conifer species, PILO and PIEN, were instead larger at lower sites, a pattern more evident for *Picea engelmannii* than *Pinus longaeva* (Fig. 2). PILO had larger cell lumens and diameters at the lower part of the western subalpine site (median la was 374 μm^2 at Sna1 and 474 μm^2 at Sna2; median cd was 25.8 μm and 27.6 μm at Sna1 and Sna2, respectively). Cellular elements of PIEN had dimensions 20–50% greater on the east side (Sna3) than on the west side (Sna1)
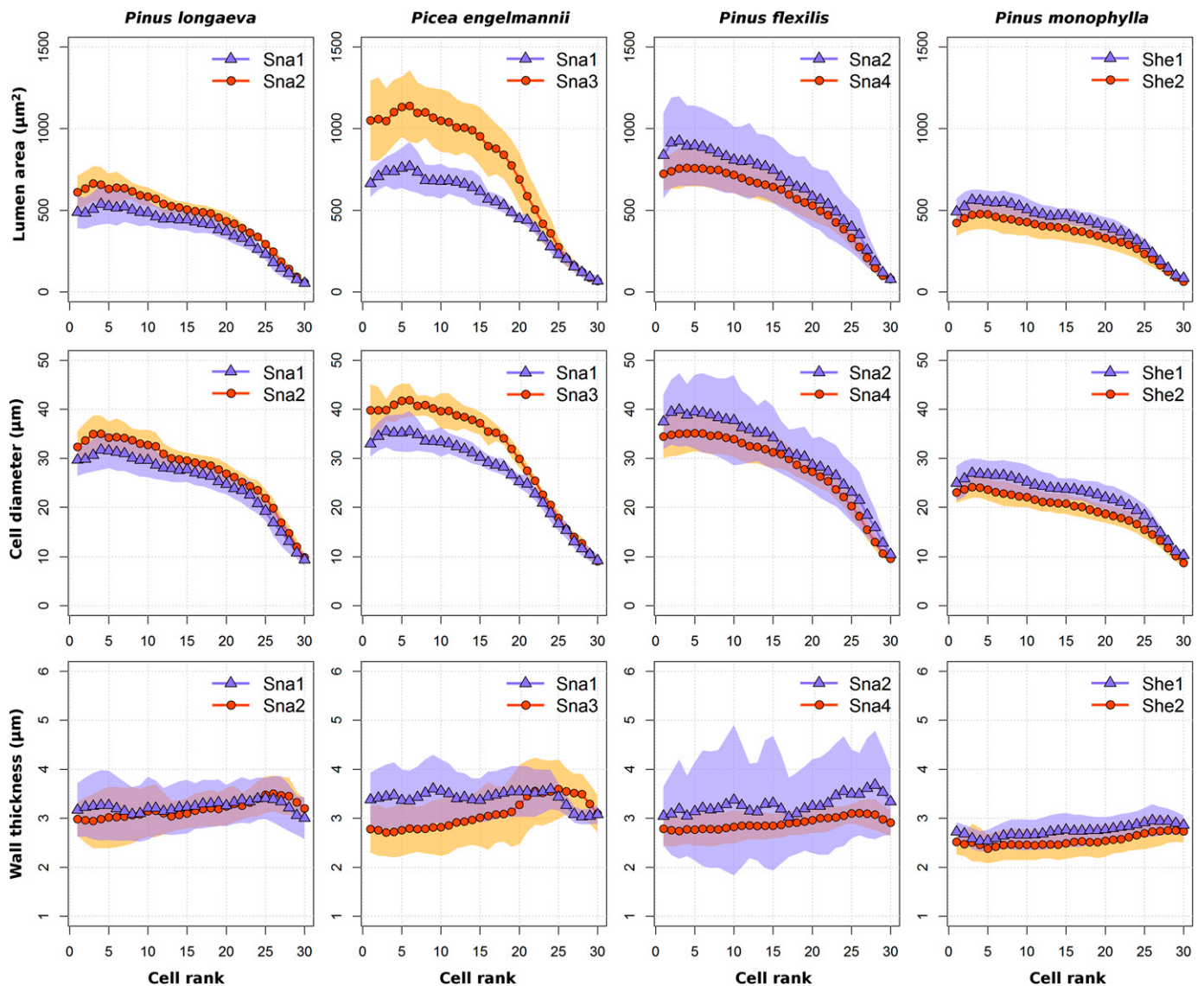

Fig. 2. Mean standardized tracheidograms of three anatomical parameters (rows) in four conifer species (columns) during the 2000–2012 period (see Table 1 for explanation of site codes). Symbols represent Tukey's biweight robust means, using blue triangles for the higher site and red circles for the lower one; color shading shows a ±1 SD interval around the means.

of the Snake Range (at Sna1 and Sna3, median la was 505 μm² and 769 μm², and median cd was 27.8 μm and 33.0 μm, respectively).

Thicker cell walls were usually found at the northern site and at higher elevations (Fig. 2). From 2000 to 2012, wall thickness of PIMO was constantly wider at the higher elevation (median wt was 2.7 μm at She1 and 2.5 μm at She2). Cell walls of PIEN tracheids were wider on the west side of the Snake Range, which was also at the higher elevation. Variability of anatomical parameters increased from the Sheep Range (south) to the Snake Range (north), while at the intraspecific level it increased with elevation. The highest annual variability was encountered in cell lumen area and radial diameter (Appendix S2).

***Earlywood and latewood tree-ring parameters*—**A significant relationship emerged between anatomical parameters of earlywood and diameter of sampled trees when considering all data, without distinctions between species (Fig. 3). Earlywood lumen area (laEW) and cell diameter (cdEW) showed the highest positive correlation with stem diameter. Earlywood wall thickness (wtEW) and all the latewood parameters showed weaker or no correlation with stem diameter (Fig. 3). Variability of tree size within a species was relatively low, making comparisons possible between populations of the same tree species growing at different elevations.

ANOVA uncovered significant differences between cell dimensions of PIEN, PILO, and PIMO (Table 3). Lumen area and cell diameter of earlywood tracheids (laEW) varied between sites for these conifer species. Wall thickness of earlywood tracheids was different for PIEN and PIMO, but not for PILO. Cellular features of latewood differed between sites only in a few cases (Table 3). Latewood lumen of PILO was smaller at Sna1 compared to Sna2. At the Sheep Range the diameter of PIMO latewood tracheids (cdLW) was narrower at the lower elevation, as was the wall thickness of both earlywood (wtEW) and latewood (wtLW) tracheids. No difference with P values ≤0.005 was found between anatomical parameters of PIFL at the Sna2 and Sna4 sites (Table 3). However, differences in PIFL cell dimensions at the higher and lower sites have increased in the most recent years (Ziaco et al., 2014).

The correlation matrix of tree-ring and anatomical parameters highlighted relationships between EW, LW, and wood anatomy (Fig. 4). For each species and site, the amount of earlywood was the best predictor of total ring width (Pearson linear coefficients always >0.90). In most species, earlywood width was directly correlated with cell diameter, and in PIFL and PIMO it was also related to lumen area (Fig. 4). Latewood width was often positively correlated with both lumen area and wall thickness. For both earlywood and latewood width, no clear latitudinal or altitudinal influences were detected.

Variation of tree-ring parameters (EW and LW) mostly agreed with those of cell dimensional features related to plant water transport (la and cd) during the years 2000–2012 (Fig. 5). Year-to-year oscillations in earlywood and latewood features were usually coherent by species, with the exception of PIEN at Sna1, where EW, LW, and their related anatomical features were negatively correlated (Fig. 5).

Wood anatomical parameters showed a decreasing trend with increasing air temperature using pooled data from all species along both NevCAN transects (Fig. 6, Appendices S3 and S4). The highest correlations were found between spring temperature and earlywood parameters (cdEW, laEW, and wtEW). A positive correlation was found between these earlywood parameters and spring precipitation. Correlations were usually stronger for cdEW (Fig. 6) compared to laEW (Appendix S3) and wtEW (Appendix S4). Latewood parameters showed similar but weaker correlations with summer temperature and precipitation, most likely because of reduced variability in cellular elements (la, cd, wt) in latewood compared to earlywood. Wall thickness in both earlywood and latewood showed weak but significant correlations with climatic variables (spring/summer temperature and precipitation; Appendix S4).

DISCUSSION

Altitudinal and latitudinal differences in climate regimes at the NevCAN sites were reflected in intra-annual wood anatomical traits, as seen in the mean tracheidograms, which portray average tree performance in response to environmental conditions. The effect of elevation was also found in tree dimension, as stem diameter generally increased from low to high elevations, especially when comparing trees of the same species. In this sense, temperature and precipitation represent ecological constraints that control plant size in the same way as they influence anatomical parameters, e.g., by determining maximum potential dimensions according to biogeoclimatic conditions (Haeussler, 2011).

A general reduction of cell lumen in the north-south direction was observed, most likely as an adaptive strategy to face drought and reduce the risk of xylem cavitation. Similar trends are found among conifer species of arid (DeSoto et al., 2011) and mesic sites of Spain (Martin-Benito et al., 2013). On the other hand, larger tracheid dimensions with increasing drought severity have been reported for *Pinus sylvestris* in the Iberian peninsula (Martín et al., 2010) and in the Alps (Eilmann et al., 2009). While Martin-Benito et al. (2013) measured tracheid lumen areas (μm²), as we did in this study, DeSoto et al. (2011), Martín et al. (2010), and Eilmann et al. (2009) based their conclusions on the radial diameter of cell lumen (μm). According to the Hagen-Poiseuille law, capillary flow rate is proportional to the fourth power of the capillary radius, hence to the square of the conduit area (Tyree and Zimmermann, 2002). This implies a disproportionate effect of lumen size on transport, so that either cell diameter or even the average of cell lumen area, which are used in studying climatic influences on wood formation (Olano et al., 2012), underestimate flow rates under the Hagen-Poiseuille law (Sperry et al., 1994).

Narrower tracheids are considered more resistant to cavitation and more efficient for hydraulic conductivity under low water availability, thanks to their higher resistance to negative pressures (Hacke and Sperry, 2001; Sperry et al., 2006). Trade-off mechanisms between hydraulic safety and structural effectiveness can be particularly complex (Tyree et al., 1994). For a given hydraulic conductivity, larger, thin-walled tracheids require a lower carbon investment in tissue production, thereby increasing the ability to tolerate water stress by reducing stomatal transpiration loss (Sperry, 2003). The reduction of both tracheid size and cell wall thickness at the southern sites and in the lower populations of PIMO and PIFL can be explained as a plastic response to drought (Bryukhanova
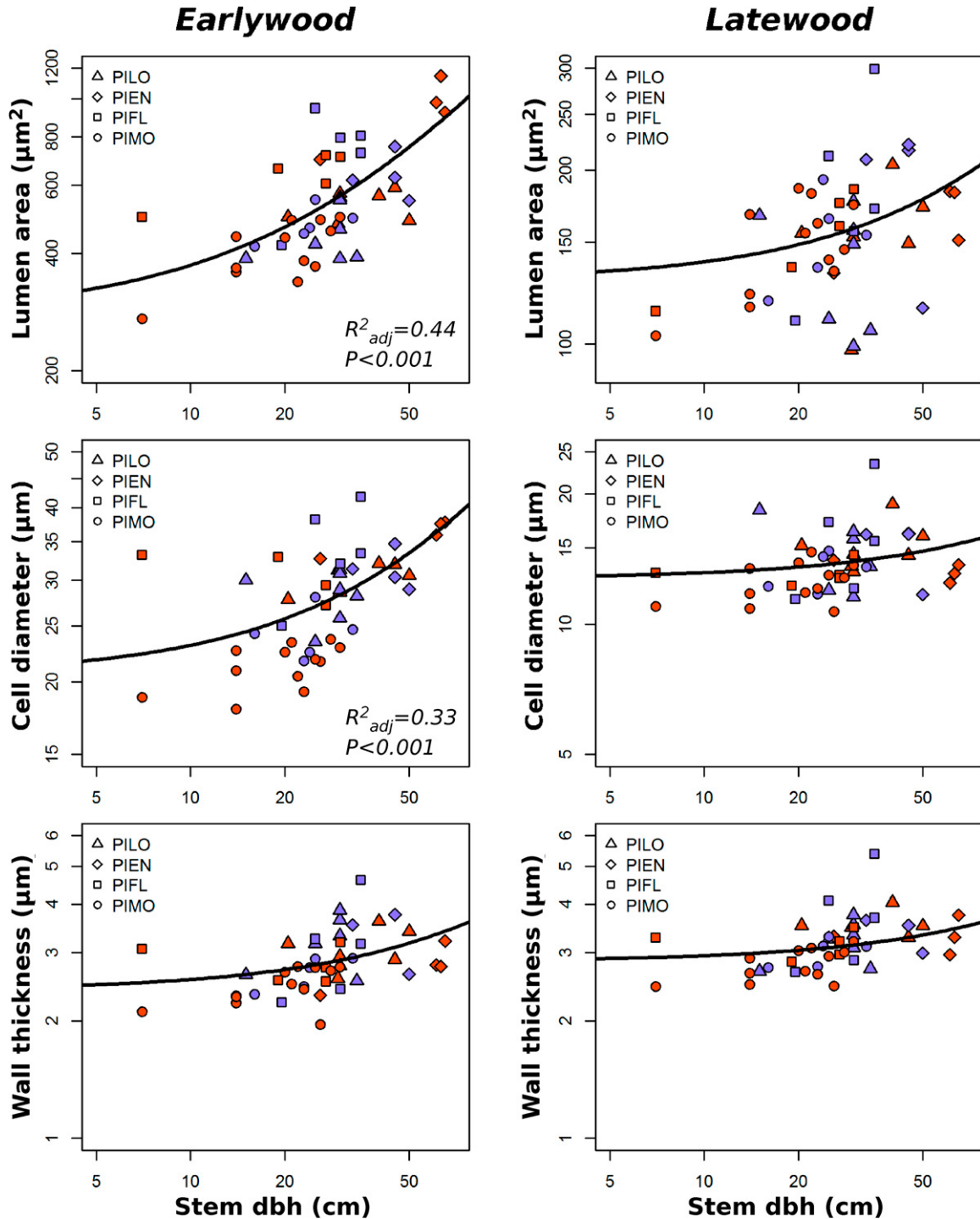
Earlywood

Latewood

Fig. 3. Relationship between tree diameter and mean anatomical features of earlywood and latewood during 2000–2012. For each conifer species, blue symbols represent trees from the higher site, and red symbols trees from the lower one. Axes are in logarithmic scale; curved lines show linear regressions on nonlinear axes. Adjusted R^2 and P values are reported only for relationships with $R^2_{adj} \geq 0.15$.

and Fonti, 2013). Water stress occurring at lower elevations during the summer may be associated with the formation of "light rings" (Panayotov et al., 2013), which are characterized by thin-walled tracheids and reduced latewood proportions (Liang et al., 1997).

The small PILO tracheids probably reflect a prevailing genetic control on wood anatomy in this species. Their change even with a minor elevation shift (larger elements in Sna2 vs. Sna1) is consistent with preliminary observations on xylogenesis that suggest an earlier onset of cambial reactivation at the

TABLE 3. *F*-statistic (with *P* value ≤ 0.005) from one-way ANOVA between mean chronologies by species of anatomical parameters for earlywood and latewood in the period 2000–2012 at the two sites where each species was present.

Species (Site)	laEW	laLW	cdEW	cdLW	wtEW	wtEW
PILO (Sna1-Sna2)	66.9 ($P < 0.001$)	11.9 ($P = 0.002$)	76.2 ($P < 0.001$)	–	–	–
PIEN (Sna1-Sna3)	98.3 ($P < 0.001$)	–	76.3 ($P < 0.001$)	–	23.2 ($P < 0.001$)	44.6 ($P < 0.001$)
PIFL (Sna2-Sna4)	–	–	–	–	–	–
PIMO (She1-She2)	9.9 ($P = 0.004$)	–	18.8 ($P < 0.001$)	9.4 ($P = 0.005$)	26.9 ($P < 0.001$)	13.6 ($P = 0.001$)

lower portion of the subalpine site (Ziaco et al., 2013). Compounding direct and indirect effects of both elevation and slope exposure could explain the larger dimension of tracheids found in PIEN on the eastern side of the Snake Range (Sna3). Based on NevCAN data, average April–June maximum temperature is 18.8°C at Sna3 and 14.9°C at Sna1-2; average April–June minimum temperature at both sites is −8.2°C. July–September rainfall accounts for about 35% of total annual precipitation at Sna3 vs. 20% at Sna1-2. Snow controls moisture availability at the Snake Range, and snowpack dynamics (e.g., timing of snowmelt) generally influence tree growth, especially at the beginning of the growing season. On the eastern flanks, higher spring temperature should anticipate snowmelt and the onset of xylem production (Rossi et al., 2011). Summer precipitation could extend the positive growth effects of the postmelting period further into the growing season, allowing the formation of larger cells. This particular climatic combination (warmer spring and moister summer) would create better growing conditions for PIEN, which in fact includes the largest individuals in our data set, particularly on the eastern flank of the Snake Range. The effect of tree size on anatomical features could be more pronounced in PIEN compared to other species included in this study, and therefore explain a larger proportion of tracheid characteristics (e.g., bigger lumen areas). Another species, PIFL, had larger tracheid lumen, diameter, and wall thickness at higher elevations in the Snake Range. Although such differences were not significant during 2000–2012, the most recent observations support this relationship (Ziaco et al., 2014).

Earlywood features accounted for most of the intraspecific anatomical differences. Earlywood width (EW) was highly correlated with total ring width at all sites. In contrast, latewood width (LW) showed less or no correlation with annual ring width at the majority of sites. High correlations between earlywood and total ring width have been reported in conifer species from temperate (Liang et al., 2013), mesic (Martin-Benito et al., 2013), and dry sites (DeSoto et al., 2011). The weaker relationship between total ring and latewood width, in particular at the Sheep Range, is consistent with an intra-seasonal climatic control of latewood formation (Wang et al., 2002), associated to the summer pluviometric regime driven by the North American Monsoon System. The correlations between lumen area and width of earlywood and latewood in Great Basin conifers suggest that dimensional features linked to moisture conditions and stem water transport (lumen area) play an important role in determining radial growth.

Normalized time series of tree-ring parameters (EW and LW) and dimensional cell features show similar variations from 2000 to 2012, suggesting the presence of a common climatic signal responsible for a large part of the interannual variability of xylem hydraulic properties and tree-ring chronologies. The strength of such signal increases from earlywood to latewood, indicating a response to water availability during the summer (Bryukhanova and Fonti, 2013). The relationship between water availability and tree-ring features that emerged along elevation gradients for two species, PIMO and PIFL, was stronger for PIMO, so that the southern sites (in the Sheep Range) show a more pronounced gradient compared to the northern ones.

Wood cellular parameters varied in response to seasonal climate, providing insights on the mechanisms of tree-ring formation, and reflecting physiological adjustments to environmental constraints. An all-species analysis of average anatomical parameters against climate indicated significant relationships of precipitation and air temperature with wood anatomy, especially in the earlywood. Weak relationships between climate and average latewood parameters, with the possible exception of cell wall thickness, could be related to the limited variability of latewood cellular features between sites. Potentially many environmental factors (e.g., soil properties, radiative balance, snowpack dynamics) might have direct and indirect effects on growth and physiological processes that produce wood anatomy and tree-ring widths. Further research will use additional anatomical and climate data as they become available over time, as well as the information from automated point dendrometers and sap flow sensors that have been installed at the NevCAN sites (Mensing et al., 2013).

In conclusion, the NevCAN elevation transects in the Great Basin enable research on environmental controls of tree growth with unprecedented detail. Results reported here provide a glimpse of the potential applications that this new scientific tool could allow in the general field of botany. While the preliminary nature of our findings and the current brevity of NevCAN time series limit our general understanding of climate–growth relationships at the cellular level, we found that differences in water stress related to elevation lead to intraspecific modifications in the anatomical structure of tree rings. These changes are likely to occur at different elevations either because of precipitation or temperature influences, or through indirect pathways that control the maximum stem size, which then affects the anatomical parameters. Annual oscillations of tree-ring and anatomical parameters highlighted the presence of a common climatic driver at the intraspecific level. When no other distinctions are considered, temperature correlations with tracheid diameter seem more important than those with precipitation, but the role and interactions of confounding factors need to be further investigated. Accomplishing this task is within reach, given the ongoing research activities related to the availability of NevCAN observations expected in the future.
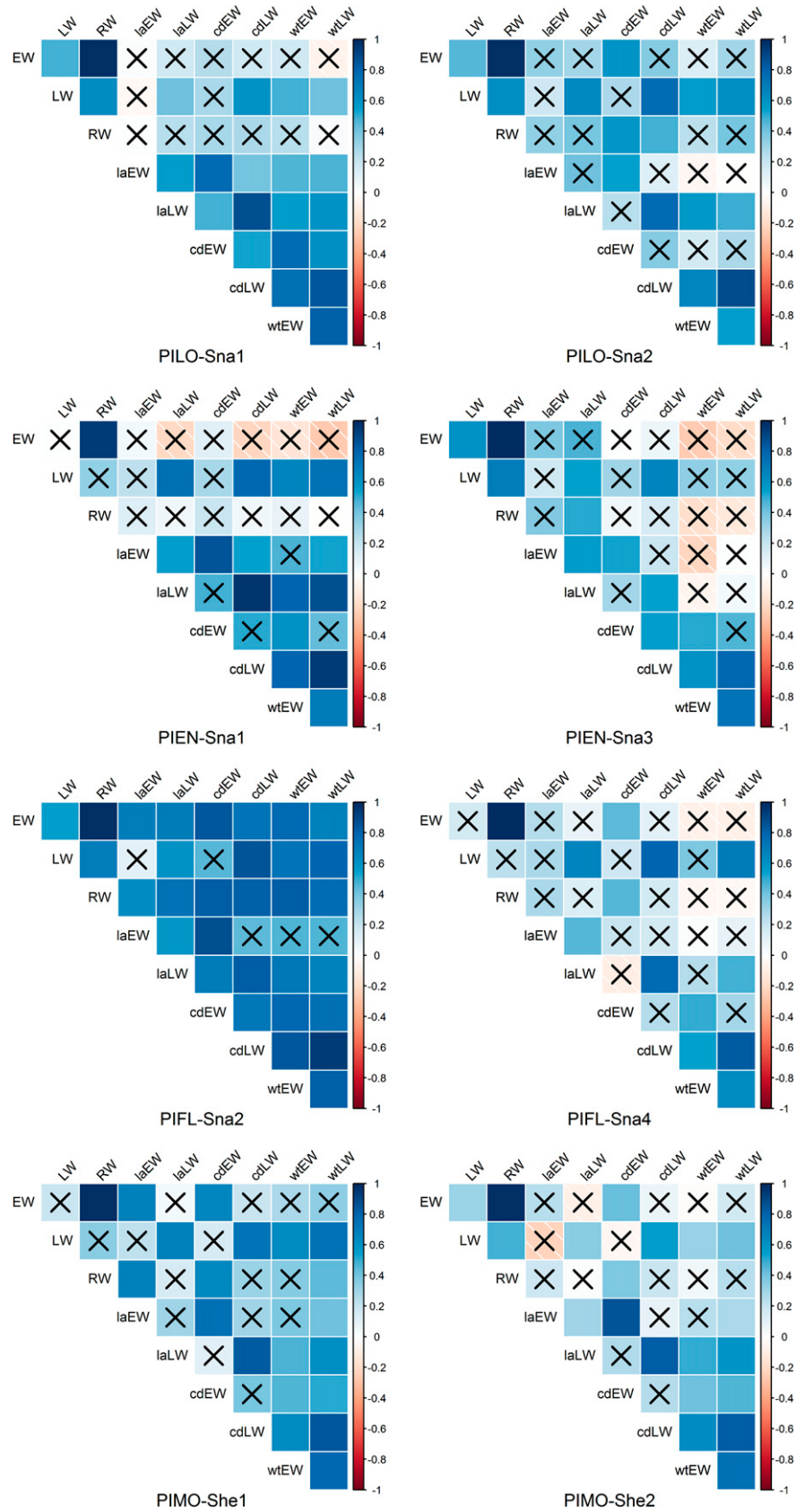
Fig. 4.   Pearson linear correlations between tree-ring (earlywood and latewood width; total ring width) and anatomical parameters. Color darkness is directly proportional to the correlation value (blue = positive correlations; red = negative correlations). Crosses mark correlations with *P* value > 0.001.
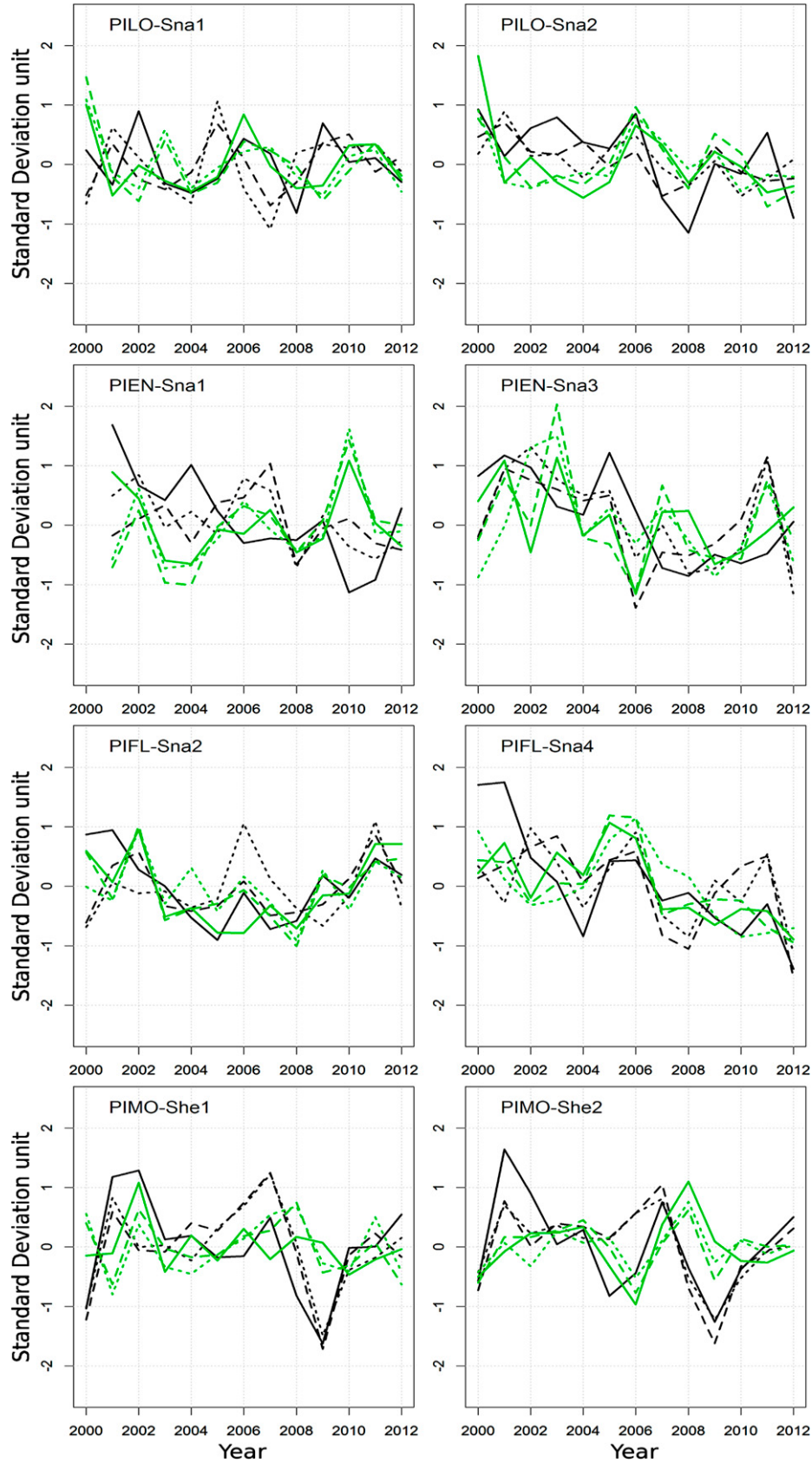
Fig. 5.   Time series of annual earlywood (black lines) and latewood (green lines) normalized (i.e., in standard deviation units) parameters during 2000–2012 plotted by species and site. Solid lines represent width, dotted lines show lumen area, and dashed lines display cell diameter.
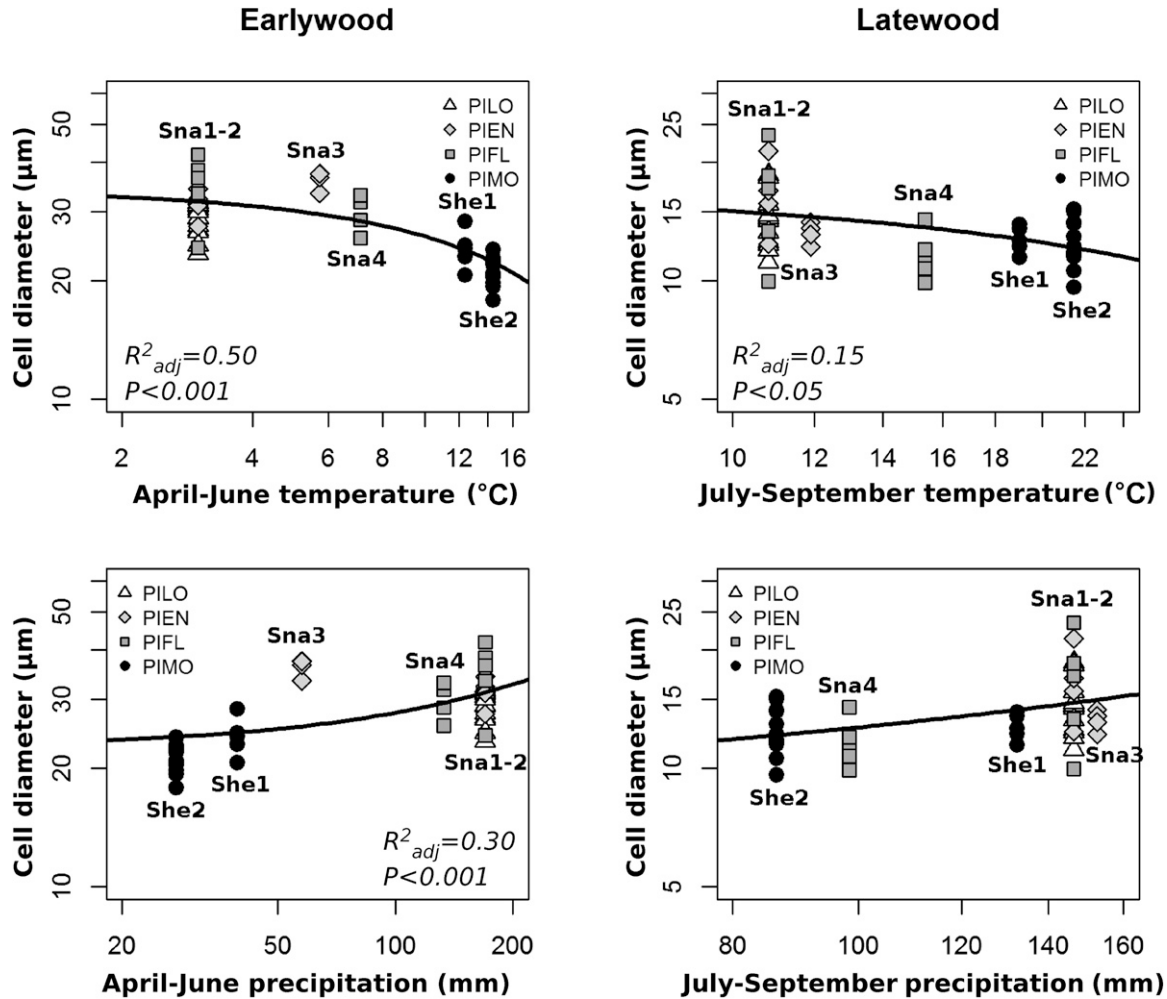
Fig. 6. Relationship between mean tracheid diameter and climatic variables (temperature and precipitation) during 2010–2012 (see Table 1 for explanation of site and species codes). Earlywood (cdEW) values were plotted against spring (April–June) mean air temperature and total precipitation. Latewood (cdLW) values were plotted against summer (July–September) mean air temperature and total precipitation. Axes are in logarithmic scale; curved lines show linear regressions on nonlinear axes. Adjusted R^2 and P values are reported only for relationships with $R^2_{adj} \geq 0.15$.

LITERATURE CITED

ADAMS, D. K., AND A. C. COMRIE. 1997. The North American monsoon. *Bulletin of the American Meteorological Society* 78: 2197–2213.

ANFODILLO, T., A. DESLAURIERS, R. MENARDI, L. TEDOLDI, G. PETIT, AND S. ROSSI. 2012. Widening of xylem conduits in a conifer tree depends on the longer time of cell expansion downwards along the stem. *Journal of Experimental Botany* 63: 837–845.

BEKKER, M. F., AND A. H. TAYLOR. 2001. Gradient analysis of fire regimes in montane forests of the southern Cascade Range, Thousand Lakes Wilderness, California, USA. *Plant Ecology* 155: 15–28.

BROWN, M. B., AND A. B. FORSYTHE. 1974. Robust tests for the equality of variances. *Journal of the American Statistical Association* 69: 364–367.

BRYUKHANOVA, M., AND P. FONTI. 2013. Xylem plasticity allows rapid hydraulic adjustment to annual climatic variability. *Trees—Structure and Function* 27: 485–496.

BUNN, A. G., M. KORPELA, F. BIONDI, F. CAMPELO, P. MÉRIAN, M. MUDELSEE, F. QEADAN, ET AL. 2014. dplR: Dendrochronology Program Library in R, version R package version 1.5.9. Website http://cran.r-project.org/web/packages/dplR/index.html [accessed 30 August 2014].

CRAUSBAY, S. D., AND S. C. HOTCHKISS. 2010. Strong relationships between vegetation and two perpendicular climate gradients high on a tropical mountain in Hawai'i. *Journal of Biogeography* 37: 1160–1174.

DE LUIS, M., K. NOVAK, J. RAVENTÓS, J. GRIČAR, P. PRISLAN, AND K. ČUFAR. 2011. Climate factors promoting intra-annual density fluctuations in Aleppo pine (*Pinus halepensis*) from semiarid sites. *Dendrochronologia* 29: 163–169.

DENNE, M. P. 1988. Definition of latewood according to Mork (1928). *IAWA Bulletin n.s.* 10: 59–62.

DESLAURIERS, A., AND H. MORIN. 2005. Intra-annual tracheid production in balsam fir stems and the effect of meteorological variables. *Trees—Structure and Function* 19: 402–408.

DESLAURIERS, A., H. MORIN, AND Y. BÉGIN. 2003. Cellular phenology of annual ring formation of *Abies balsamea* in the Quebec boreal forest (Canada). *Canadian Journal of Forest Research* 33: 190–200.

DESLAURIERS, A., S. ROSSI, T. ANFODILLO, AND A. SARACINO. 2008. Cambial phenology, wood formation and temperature thresholds in two contrasting years at high altitude in southern Italy. *Tree Physiology* 28: 863–871.

DESOTO, L., M. DE LA CRUZ, AND P. FONTI. 2011. Intra-annual patterns of tracheid size in the Mediterranean tree *Juniperus thurifera* as an indicator of seasonal water stress. *Canadian Journal of Forest Research* 41: 1280–1294.

DI FILIPPO, A., F. BIONDI, K. ČUFAR, M. DE LUIS, M. GRABNER, M. MAUGERI, E. PRESUTTI SABA, ET AL. 2007. Bioclimatology of beech (*Fagus sylvatica* L.) in the Eastern Alps: Spatial and altitudinal climatic signals identified through a tree-ring network. *Journal of Biogeography* 34: 1873–1892.

Douglass, A. E. 1941. Crossdating in dendrochronology. *Journal of Forestry* 39: 825–831.

Eilmann, B., R. Zweifel, N. Buchmann, P. Fonti, and A. Rigling. 2009. Drought-induced adaptation of the xylem in Scots pine and pubescent oak. *Tree Physiology* 29: 1011–1020.

Fonti, P., G. von Arx, I. García-González, B. Eilmann, U. Sass-Klaassen, H. Gärtner, and D. Eckstein. 2010. Studying global change through investigation of the plastic responses of xylem anatomy in tree rings. *New Phytologist* 185: 42–53.

Foster, T. E., and J. R. Brooks. 2001. Long-term trends in growth of *Pinus palustris* and *Pinus elliottii* along a hydrological gradient in central Florida. *Canadian Journal of Forest Research* 31: 1661–1670.

Franceschini, T., F. Longuetaud, J.-D. Bontemps, O. Bouriaud, B.-D. Caritey, and J.-M. Leban. 2013. Effect of ring width, cambial age, and climatic variables on the within-ring wood density profile of Norway spruce *Picea abies* (L.) Karst. *Trees—Structure and Function* 27: 913–925.

Fritts, H. C. 2001. Tree rings and climate [reprint of the 1976 ed.]. The Blackburn Press, Caldwell, New Jersey, USA.

Fritts, H. C., D. G. Smith, J. W. Cardis, and C. A. Budelsky. 1965. Tree-ring characteristics along a vegetation gradient in northern Arizona. *Ecology* 46: 393–401.

Galván, J. D., J. J. Camarero, G. Sangüesa-Barreda, A. Q. Alla, and E. Gutiérrez. 2012. Sapwood area drives growth in mountain conifer forests. *Journal of Ecology* 100: 1233–1244.

Grayson, D. K. 2011. The Great Basin: A natural prehistory, revised ed. University of California Press, Berkeley, California, USA.

Griffin, R. D., C. A. Woodhouse, D. M. Meko, D. W. Stahle, H. L. Faulstich, C. Carrillo, R. Touchan, et al. 2013. North American monsoon precipitation reconstructed from tree-ring latewood. *Geophysical Research Letters* 40: 954–958.

Guay, R. 2013. WinCELL 2013 for wood cell analysis. Regent Instruments Inc., Quebec City, Quebec, Canada.

Hacke, U. G., and J. S. Sperry. 2001. Functional and ecological xylem anatomy. *Perspectives in Plant Ecology, Evolution and Systematics* 4: 97–115.

Haeussler, S. 2011. Rethinking biogeoclimatic ecosystem classification for a changing world. *Environmental Reviews* 19: 254–277.

Holeksa, J., M. Saniga, J. Szwagrzyk, T. Dziedzic, S. Ferenc, and M. Wodka. 2007. Altitudinal variability of stand structure and regeneration in the subalpine spruce forests of the Pol'ana biosphere reserve, Central Slovakia. *European Journal of Forest Research* 126: 303–313.

Houghton, J. G., C. M. Sakamoto, and R. O. Gifford. 1975. Nevada's weather and climate. Nevada Bureau of Mines and Geology, University of Nevada, Reno, Nevada, USA.

Johnson, B. G., P. S. J. Verburg, and J. A. Arnone III. 2014. Effects of climate and vegetation on soil nutrients and chemistry in the Great Basin studied along a latitudinal-elevational climate gradient. *Plant and Soil* 382: 151–163.

Keenan, T. F., J. Gray, M. A. Friedl, M. Toomey, G. Bohrer, D. Y. Hollinger, J. W. Munger, et al. 2014. Net carbon uptake has increased through warming-induced changes in temperate forest phenology. *Nature Climate Change* 4: 598–604.

King, G. M., P. Fonti, D. Nievergelt, U. Büntgen, and D. C. Frank. 2013. Climatic drivers of hourly to yearly tree radius variations along a 6°C natural warming gradient. *Agricultural and Forest Meteorology* 168: 36–46.

Krause, C., S. Rossi, M. Thibeault-Martel, and P.-Y. Plourde. 2010. Relationships of climate and cell features in stems and roots of black spruce and balsam fir. *Annals of Forest Science* 67: 402.

LaMarche, V. C., Jr. 1974. Frequency-dependent relationships between tree-ring series along an ecological gradient and some dendroclimatic implications. *Tree-Ring Bulletin* 34: 1–20.

Liang, C., L. Filion, and L. Cournoyer. 1997. Wood structure of biotically and climatically induced light rings in eastern larch (*Larix laricina*). *Canadian Journal of Forest Research* 27: 1538–1547.

Liang, W., I. Heinrich, S. Simard, G. Helle, I. D. Liñán, and T. Heinken. 2013. Climate signals derived from cell anatomy of Scots pine in NE Germany. *Tree Physiology* 33: 833–844.

Martín, J. A., L. G. Esteban, P. de Palacios, and F. G. Fernández. 2010. Variation in wood anatomical traits of *Pinus sylvestris* L. between Spanish regions of provenance. *Trees—Structure and Function* 24: 1017–1028.

Martin-Benito, D., H. Beeckman, and I. Cañellas. 2013. Influence of drought on tree rings and tracheid features of *Pinus nigra* and *Pinus sylvestris* in a mesic Mediterranean forest. *European Journal of Forest Research* 132: 33–45.

Mensing, S. A., S. D. J. Strachan, J. A. Arnone III, L. F. Fenstermaker, F. Biondi, D. A. Devitt, B. G. Johnson, et al. 2013. A network for observing Great Basin climate change. *Eos (Transactions of the American Geophysical Union)* 94: 105–106.

Mosteller, F., and J. W. Tukey. 1977. Data analysis and regression. Addison-Wesley, Reading, Massachusetts, USA.

Olano, J. M., M. Eugenio, A. I. García-Cervigón, M. Folch, and V. Rozas. 2012. Quantitative tracheid anatomy reveals a complex environmental control of wood structure in continental Mediterranean climate. *International Journal of Plant Sciences* 173: 137–149.

Padien, D. J., and K. Lajtha. 1992. Plant spatial pattern and nutrient distribution in pinyon-juniper woodlands along an elevational gradient in northern New Mexico. *International Journal of Plant Sciences* 153: 425–433.

Panayotov, M. P., N. Zafirov, and P. Cherubini. 2013. Fingerprints of extreme climate events in *Pinus sylvestris* tree rings from Bulgaria. *Trees—Structure and Function* 27: 211–227.

Peñuelas, J., and M. Boada. 2003. A global change-induced biome shift in the Montseny mountains (NE Spain). *Global Change Biology* 9: 131–140.

R Development Core Team. 2012. R: A language and environment for statistical computing, version 2.15.0. Website: http://www.R-project.org [accessed 8 September 2014].

Raich, J. W., A. E. Russell, and P. M. Vitousek. 1997. Primary productivity and ecosystem development along an elevational gradient on Mauna Loa, Hawai'i. *Ecology* 78: 707–721.

Reinhardt, K., C. Castanha, M. J. Germino, and L. M. Kueppers. 2011. Ecophysiological variation in two provenances of *Pinus flexilis* seedlings across an elevation gradient from forest to alpine. *Tree Physiology* 31: 615–625.

Rossi, S., T. Anfodillo, and R. Menardi. 2006. Trephor: A new tool for sampling microcores from tree stems. *IAWA Journal* 27: 89–97.

Rossi, S., H. Morin, and A. Deslauriers. 2011. Multi-scale influence of snowmelt on xylogenesis of black spruce. *Arctic, Antarctic, and Alpine Research* 43: 457–464.

Rossi, S., T. Anfodillo, K. Čufar, H. E. Cuny, A. Deslauriers, P. Fonti, D. C. Frank, et al. 2013. A meta-analysis of cambium phenology and growth: Linear and non-linear patterns in conifers of the northern hemisphere. *Annals of Botany* 112: 1911–1920.

Rossi, S., M.-J. Girard, and H. Morin. 2014a. Lengthening of the duration of xylogenesis engenders disproportionate increases in xylem production. *Global Change Biology* 20: 2261–2271.

Rossi, S., E. Cairo, C. Krause, and A. Deslauriers. 2014b. Growth and basic wood properties of black spruce along an alti-latitudinal gradient in Quebec, Canada. *Annals of Forest Science* doi:10.1007/s13595-014-0399-8.

Sistla, S. A., J. C. Moore, R. T. Simpson, L. Gough, G. R. Shaver, and J. P. Schimel. 2013. Long-term warming restructures Arctic tundra without changing net soil carbon storage. *Nature* 497: 615–618.

Speer, J. H. 2010. Fundamentals of tree-ring research. University of Arizona Press, Tuscon, Arizona, USA.

Sperry, J. S. 2003. Evolution of water transport and xylem structure. *International Journal of Plant Sciences* 164: S115–S127.

Sperry, J. S., K. L. Nichols, J. E. M. Sullivan, and S. E. Eastlack. 1994. Xylem embolism in ring-porous, diffuse-porous, and coniferous trees of northern Utah and interior Alaska. *Ecology* 75: 1736–1752.

Sperry, J. S., U. G. Hacke, and J. Pittermann. 2006. Size and function in conifer tracheids and angiosperm vessels. *American Journal of Botany* 93: 1490–1500.

St-Germain, J.-L., and C. Krause. 2008. Latitudinal variation in tree-ring and wood cell characteristics of *Picea mariana* across the continuous boreal forest in Quebec. *Canadian Journal of Forest Research* 38: 1397–1405.

STAHLE, D. W., M. K. CLEAVELAND, H. D. GRISSINO-MAYER, R. D. GRIFFIN, F. K. FYE, M. D. THERRELL, D. J. BURNETTE, ET AL. 2009. Cool- and warm-season precipitation reconstructions over western New Mexico. *Journal of Climate* 22: 3729–3750.

STEPHENSON, N. L., AND P. J. VAN MANTGEM. 2005. Forest turnover rates follow global and regional patterns of productivity. *Ecology Letters* 8: 524–531.

TYREE, M. T., AND M. H. ZIMMERMANN. 2002. Xylem structure and the ascent of sap, 2nd ed. Springer-Verlag, Berlin, Germany.

TYREE, M. T., S. D. DAVIS, AND H. COCHARD. 1994. Biophysical perspectives of xylem evolution: Is there a tradeoff of hydraulic efficiency for vulnerability to dysfunction? *IAWA Journal* 15: 335–360.

VAGANOV, E. A. 1990. The tracheidogram method in tree-ring analysis and its application. *In* E. R. Cook and L. A. Kairiukstis [eds.], Methods of dendrochronology, 63–76. Kluwer, Dordrecht, The Netherlands.

VAGANOV, E. A., M. K. HUGHES, AND A. V. SHASHKIN. 2006. Growth dynamics of conifer tree rings: Images of past and future environments. Springer, New York, New York, USA.

VAN DER MAATEN-THEUNISSEN, M., AND O. BOURIAUD. 2012. Climate–growth relationships at different stem heights in silver fir and Norway spruce. *Canadian Journal of Forest Research* 42: 958–969.

VIEIRA, J., F. CAMPELO, AND C. NABAIS. 2009. Age-dependent responses of tree-ring growth and intra-annual density fluctuations of *Pinus pinaster* to Mediterranean climate. *Trees—Structure and Function* 23: 257–265.

WANG, L., S. PAYETTE, AND Y. BÉGIN. 2002. Relationships between anatomical and densitometric characteristics of black spruce and summer temperature at tree line in northern Quebec. *Canadian Journal of Forest Research* 32: 477–486.

WHITTAKER, R. H. 1967. Gradient analysis of vegetation. *Biological Reviews of the Cambridge Philosophical Society* 42: 207–264.

ZIACO, E., F. BIONDI, S. ROSSI, AND A. DESLAURIERS. 2013. Quantifying cambial activity of high-elevation conifers in the Great Basin, Nevada, USA, Fall Meeting, Abstract ID 1795104. American Geophysical Union, San Francisco, California, USA.

ZIACO, E., F. BIONDI, S. ROSSI, AND A. DESLAURIERS. 2014. Intra-annual wood anatomical features of high-elevation conifers in the Great Basin, USA. *Dendrochronologia* in press http://dx.doi.org/10.1016/j.dendro.2014.07.006.